February 2009

Max Planck Institute for Solar System Research
Y. Narita, M. Fränz, N. Krupp with assistants
A. Angsmann, L. Guicking, K. Hallgren, and P. Kobel

Exercise for Sun-Planet Connections (2009) - Part 1

Space Weather

1.1 Space weather influence on spacecraft

Discuss what different effects space weather might have on spacecraft (and humans) in orbit around earth. Consider also the impact of different orbital parameters and if the spacecraft move to an interplanetary trajectory.

1.2 Parker spiral

(a) The solar wind plasma carries magnetic field lines with it, which attain a spiral shape due to the solar rotation as they extend through the solar system. This is the so-called *Parker spiral*.
Derive an equation which describes the flow of this plasma, assuming that it emerges from the solar surface ($r = r_0$) at the equator in radial direction (at the speed v) from a point at an arbitrary solar longitude ϕ_0. Write down two time-dependent equations in polar coordinates which describe the outward movement of this plasma in r and ϕ direction. Then combine these formulas to find a time-independent description for r, depending on v, ϕ, ϕ_0, r_0 and the angular velocity Ω of the solar rotation.

The resulting equation for r is a so-called *Archimedean spiral* (general form: $r = a+b\phi$ with real numbers a, b) which has the property that the distance between successive turnings of the spiral is always constant.

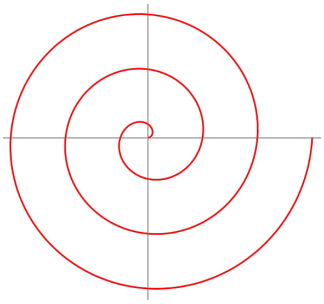

Figure 1: One arm of an Archimedean spiral.

(b) The aim of this exercise is to derive an equation in polar coordinates which relates the components B_r and B_ϕ to each other, depending on the radial distance r from the Sun, the radial velocity v_r of the solar wind and the Sun's angular velocity Ω. This will show us how far the magnetic field lines twist as they move outward with the plasma. For simplicity, stay within the equatorial plane, thus $B_\theta = v_\theta = 0$.

First, show that the fact that magnetic fields are source-free leads to the equation

$$B_r = B_0 \cdot \frac{r_0^2}{r^2} \tag{1}$$

where B_0 represents the magnetic field at r_0 (boundary condition). Next, assume a steady flow ($\vec{B}$ does not change with time) and use the generalized Ohm's law as well as Faraday's law to prove that

$$r\left(v_\phi B_r - v_r B_\phi\right) = \text{const.} \tag{2}$$

With $v_{\phi_0} = r_0\Omega$ and the assumption that the initial magnetic field emerging from the sun is purely radial, derive an equation for B_ϕ, depending only on B_r, v_r, v_ϕ, r and Ω (start from equation (2) and use equation (1) to eliminate B_0 and r_0). You can then further simplify the resulting equation for large distances from the Sun, where $r\Omega \gg v_\phi$.

Hints:

- *Divergence of a vector field $\vec{F}$ in spherical coordinates:*

$$\vec{\nabla}\cdot\vec{F} = \frac{1}{r^2}\frac{\partial}{\partial r}\left(r^2 F_r\right) + \frac{1}{r\sin\theta}\frac{\partial}{\partial\theta}\left(F_\theta \sin\theta\right) + \frac{1}{r\sin\theta}\frac{\partial F_\phi}{\partial\phi} \tag{3}$$

- *Curl of a vector field $\vec{F}$ in spherical coordinates:*

$$\begin{aligned}\vec{\nabla}\times\vec{F} \;=\; & \frac{1}{r\sin\theta}\left(\frac{\partial}{\partial\theta}\left(F_\phi\sin\theta\right) - \frac{\partial F_\theta}{\partial\phi}\right)\hat{r} + \frac{1}{r}\left(\frac{1}{\sin\theta}\frac{\partial F_r}{\partial\phi} - \frac{\partial}{\partial r}\left(rF_\phi\right)\right)\hat{\theta} \\ & + \frac{1}{r}\left(\frac{\partial}{\partial r}\left(rF_\theta\right) - \frac{\partial F_r}{\partial\theta}\right)\hat{\phi}\end{aligned}$$

- *Generalized Ohm's law: $\vec{j} = \sigma\left(\vec{E} + \vec{v}\times\vec{B}\right)$, where $\sigma \to \infty$ in this case, as the conductivity of plasmas is very high*
- *Faraday's law: $\frac{\partial\vec{B}}{\partial t} = -\vec{\nabla}\times\vec{E}$*
- *we are regarding an axially symmetric system in $\hat{\phi}$, thus $\frac{\partial\vec{v}}{\partial\phi} = \frac{\partial\vec{B}}{\partial\phi} = 0$*

(c) Using the equation derived in part (b) and assuming a constant radial solar wind particle velocity of $\approx$ 400 km/s, calculate the angle of the interplanetary magnetic field lines (compared to the radial direction) at the orbit of the Earth (1 AU = $1.5{\cdot}10^{11}$ m). The sidereal rotation period of the Sun at the equator is 25.05 days.

Which value does this angle approach for very large distances from the Sun?

1.3 Electric power input

How large is the electric power input from the solar wind to the Earth magnetosphere (see figure below)? Use the values of $v = 400\,[\text{km/s}]$ (solar wind speed), $B = 5\,[\text{nT}]$ (interplanetary magnetic field), and the radius $R = 10\,\text{R}_\text{E}$ for the magnetosphere cross section. Hint: The Poynting flux $\vec{S} = \frac{1}{\mu_0}\vec{E}\times\vec{B}$ [W/m^2] gives an estimate of electric power. $R_E = 6400$ km, $\mu_0 = \frac{1}{4\pi}\cdot 10^{-4}\frac{\text{H}}{\text{m}}$

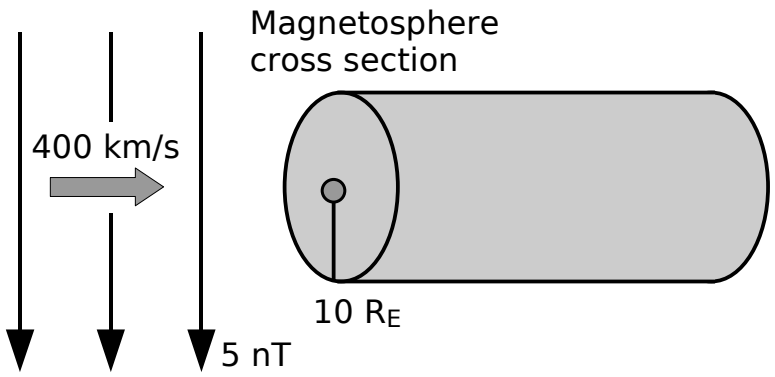

Figure 2: Cylinder magnetosphere in a plasma flow.

1.4 Induced voltage

1994 an space tether experiment was flown on the Space Shuttle. Estimate the induced voltage potential on a tether attached to the space shuttle. The experiment in question took place at an altitude of 300 km and with an orbital inclination of 28°.

February 2009

Max Planck Institute for Solar System Research
Y. Narita, M. Fränz, N. Krupp with assistants
A. Angsmann, L. Guicking, K. Hallgren, and P. Kobel

Solutions to Exercise Sun-Planet Connections (2009)

Space Weather

1.1 Space weather influence on spacecraft

Spacecraft anomalies are grouped into broad categories based upon the effect on the spacecraft, see below for a list of the categories. An in–depth explanation of each effect will follow the list. For manned space flight, the radiation dose is the major obstacle, and the overall health of the space ship.

Radiation effects on humans are similar to the effects on electronics. Dose effects affect all cells, especially those which are not (or slowly) renewed. Single energetic particles can also break the DNA chain in the cell nucleus, producing chromosome abberations, translocations and tumours. They can induce cell mutations that can have an impact on the genetics.

All the mentioned effects increase as a spacecraft leaves the protective magnetosphere of the earth. Repetitive travel through radiation belts will be of more harm than continuous travel through interplanetary space due to the trapped high-energy particles.

Surface charging
Deep dielectric, or bulk charging
Single Event Upset (SEU), a) Galactic cosmic rays and b) Solar Proton events
Spacecraft drag (<1000 km)
Total dose effects
Solar radio frequency interference and telemetry scintillation
Spacecraft orientation
Photonics noise

Surface charging

Surface charging to a high voltage does not usually cause immediate problems for a spacecraft. However, electrical discharges resulting from differential charging can damage surface material and create electromagnetic interference that can result in damage to electronic devices. Variations in low-energy plasma parameters around the spacecraft, along with the photoelectric effect from sunlight, cause most surface charging. Due to the low energy of the plasma, this type of

charging does not penetrate directly into interior components. Surface charging can be largely mitigated through proper material selection and grounding techniques.

Surface charging occurs predominantly during geomagnetic storms. It is usually more severe in the spacecraft local times of midnight to dawn but can occur at any time. Night to day, and day to night transitions are especially problematic during storms since the photoelectric effect is abruptly present or absent, which can trip discharges. Additionally, thruster firings can change the local plasma environment and trigger discharges.

Deep dielectric, or bulk charging

This phenomenon is a problem primarily for high altitude spacecraft. At times when the Earth is immersed in a high-speed solar wind stream, the Van Allen belts become populated with high fluxes of relativistic ($>\approx$1 MeV) electrons. These electrons easily penetrate spacecraft shielding and can build up charge where they come to rest in dielectrics such as coax cables, circuit boards, electrically floating radiation shields, etc. If the electron flux is high for extended periods, abrupt discharges (tiny "lightening strokes") deep in the spacecraft can occur.

High fluxes of these electrons vary with the 11-year solar cycle and are most prevalent late in the cycle and at solar minimum. Occasionally, high-energy electron events recur with a 27-day periodicity - the rotation period of the Sun. Discharges appear to correlate well with long periods of high fluxes. At these times, charge buildup exceeds the natural charge leakage rate of the dielectric. The charge builds and discharge occurs after the breakdown voltage is reached. In the past, some energetic electron enhancements at GEO have approached two weeks in duration. It was at the end of one of these long-duration enhancements in 1994 that two Canadian satellites experienced debilitating upsets.

Historically, deep dielectric discharges begin to occur when the >2 MeV fluxes exceed 1000 particles/cm/sec/ster. In general, fluxes become elevated for all GEO (Geostationary Orbit) spacecraft at the same time. However, there is a diurnal variation where fluxes peak by approximately an order of magnitude for spacecraft at local noon.

Single Event Upset (SEU), a) Galactic cosmic rays and b) Solar Proton events.

Single event upsets occur when a high-energy particle ($>\approx$50 MeV) penetrates spacecraft shielding and has the misfortune to hit a device in just the wrong way to cause disruption. This is generally a hit or miss situation. Effects can range from simple device tripping to component latch-up or failure. Particle bombardment of memory devices can also change on-board software through physical damage or through deposition of charge resulting in a "bit flip." There are two natural phenomena that cause this type of problem - Galactic Cosmic Rays (GCRs) and Solar Proton Events (SPEs).

Galactic cosmic "rays" are actually particles, sometimes with high Z number (nuclear mass) and energies exceeding GeV levels. Fortunately, the flux of GCRs is relatively low so the resulting SEU rate is also low. GCR fluxes are highest by approximately 25% during solar minimum. It is at this time that the Sun expels little solar material and magnetic fields to detect the incoming GCRs prior to arrival at Earth.

Solar Proton Events at Earth can occur throughout the solar cycle but are most frequent in solar maximum years. SPEs result from powerful solar flares with fast coronal mass ejections. During an SPE satellites experience dramatically increased bombardment by high-energy particles, primarily protons. Fluxes of particles with energies >10 MeV, can reach 70,000 protons/cm2/sec/ster. SEU rates increase with high fluxes since there is a higher likelihood of impact with a sensitive location. High-energy particles reach Earth from 30 minutes to several hours following the initiating solar event. The particle energy spectrum and arrival time seen by satellites varies with the location and nature of the event on the solar disk.

Spacecraft drag (<1000 km)

Spacecraft in LEO (Low Earth Orbit) experience periods of increased drag that causes them to slow, lose altitude and finally reenter the atmosphere. Short-term drag effects are generally felt by spacecraft <1,000 km altitude. Drag increase is well correlated with solar Ultraviolet (UV) output and additional atmospheric heating that occurs during geomagnetic storms. Solar UV flux varies in concert with the 11-year solar cycle and to a lesser degree with the 27-day solar rotation period. Geomagnetic storms are sporadic, but most major storms occur during solar maximum years. During the great geomagnetic storm of 13-14 March 1989, tracking of thousands of space objects was lost and it took North American Defense Command (NORAD) many days to reacquire them in their new, lower, faster orbits. One LEO satellite lost over 30 kilometers of altitude, and hence significant lifetime, during this storm.

Total dose effects

Spacecraft "age" through continual bombardment by GCRs, trapped radiation, and SPEs. There are several models used to estimate the total dose expected in various orbits and at different stages of the solar cycle. These models provide total dose estimates that are helpful in estimating the lifetime of an operational satellite. The total dose a satellite receives from GCRs is relatively constant. Solar cycle variations in trapped radiation are also reasonably well modeled. SPEs are most prevalent during the solar maximum years but their time of occurrence and severity are very difficult to model.

Spacecraft components are manufactured to withstand high total doses of radiation. However, it is important for the satellite operator to know how much dose each spacecraft in his fleet has endured. This knowledge allows for reasoned replacement strategies in an industry with very long manufacturing lead times.

Spacecraft power panels are physically and permanently damaged by particles of energy high enough to penetrate their surfaces. During one large high-energy SPE, several percent of power panel output can be lost. This shortens the overall lifetime of the spacecraft or at least entails power management problems as the spacecraft nears its end of life. Recent developments in the manufacturing process have made SPEs less of a problem, but power loss still occurs in these new panels.

Solar radio frequency interference and telemetry scintillation

The Sun is a strong, highly variable, broad-band radio source. At times, the Sun is within a side-lobe or even the main beam of a ground antenna looking at a satellite, usually pointed within about 1 degree of the Sun. If the Sun happens to produce a large radio burst during that time, the signal from the spacecraft can be overwhelmed. Large solar radio bursts occur most frequently during solar maximum years. An operator should be aware of when the Sun is in close proximity to the satellite being tracked.

At times, the ionosphere becomes highly irregular causing satellite signals to band inhomogeneously when they transit this disturbed medium, and scintillate at the receiver. Strong geomagnetic storms can cause scintillation in the auroral zones. Additionally, scintillation is problematic for signals traversing the equatorial ionosphere. In this area, large rising turbulent plumes form in the afternoon and evening ionosphere, resulting in rapidly varying, significant signal loss. Not only does this affect telemetry up/downlink, but GPS users can lose tracking of enough spacecraft so as to make location finding difficult.

Spacecraft orientation

Some spacecraft use Earth's magnetic field as an aid in orientation or as a force to work against to dump momentum and slow down reaction wheels. During geomagnetic storms, dramatic unexpected changes in the magnetic field observed by the satellite can lead to mis-orientation of the spacecraft.

GEO spacecraft also experience a unique occurrence termed a Magnetopause Crossing. The sunward boundary of Earth's magnetic field (magnetopause) is usually located approximately 10 Earth radii from Earth center. Variations in the pressure (due to changes in the velocity, density, and magnetic field) of the incoming solar wind change the location of that boundary. Under solar wind conditions of high velocity and density and strongly southward magnetic field, this boundary can be rammed to inside the altitude of GEO orbit at 6.6 Earth radii. A GEO spacecraft on the sunward side of Earth can be outside the (compressed) magnetopause and in the (modified) solar wind magnetic field for minutes to hours. When the magnetopause is inside 6.6 radii, GEO spacecraft are within the magnetosheath between the bow shock and the magnetopause. Magnetic sensors on board become confused as the detected magnetic field drops from $\approx$200 nT to near zero and its sign changes erratically.

During the great solar storm 1989 some satellites got so disorientated that they turned upside-down.

Photonics noise

During Solar Proton Events, photonic devices such as CCDs and some star trackers experience a noise floor increase. For star trackers, this noise can result in orientation problems. Streaks and extra "photo electrons" in imaging CCDs can compromise data quality.

1.2 Parker spiral

(a) For the radial plasma outflow from the Sun at a speed v, we have

$$r = v \cdot t + r_0 \tag{1}$$

where t is the time and r_0 the radius of the Sun. Furthermore, due to the solar rotation at the angular velocity Ω, the plasma moves in ϕ direction according to

$$\phi = \Omega \cdot t + \phi_0 \tag{2}$$

where ϕ stands for the solar longitude of the point from which the plasma originates. This leads to the time-independent equation

$$r = v \cdot \frac{\phi - \phi_0}{\Omega} + r_0 \tag{3}$$

which describes the plasma distribution in polar coordinates.

(b) As the magnetic field lines are carried along with the solar wind, they also have the same shape as the plasma distribution, an Archimedean spiral. To derive this, we remain in the equatorial plane, thus $\vec{v} = (v_r, 0, v_\phi)$ and $\vec{B} = (B_r, 0, B_\phi)$.

The magnetic field is source-free: $\vec{\nabla} \cdot \vec{B} = 0$, which transforms to

$$\frac{1}{r^2}\frac{\partial}{\partial r}\left(r^2 B_r\right) + \frac{1}{r\sin\theta}\frac{\partial}{\partial\theta}\left(B_\theta \sin\theta\right) + \frac{1}{r\sin\theta}\frac{\partial B_\phi}{\partial\phi} = 0 \tag{4}$$

in spherical coordinates. But in this case, $B_\theta = 0$ and $\frac{\partial}{\partial\phi} = 0$, thus the second and third term disappear, so that

$$\frac{1}{r^2}\frac{\partial}{\partial r}\left(r^2 B_r\right) = 0 \tag{5}$$

$$\Rightarrow r^2 B_r = r_0^2 B_0 = \text{const.} \tag{6}$$

$$\Rightarrow B_r = B_0 \cdot \frac{r_0^2}{r^2} \tag{7}$$

We can now use the generalized Ohm's law

$$\vec{j} = \sigma\left(\vec{E} + \vec{v} \times \vec{B}\right) \tag{8}$$

$$\Rightarrow \vec{E} = -\vec{v} \times \vec{B} + \vec{j}/\sigma \approx -\vec{v} \times \vec{B} \tag{9}$$

because the conductivity of plasmas is very high ($\sigma \to \infty$). Together with Faraday's law

$$\frac{\partial \vec{B}}{\partial t} = -\vec{\nabla} \times \vec{E} \tag{10}$$

we get

$$\frac{\partial \vec{B}}{\partial t} = \vec{\nabla} \times \left(\vec{v} \times \vec{B}\right) \tag{11}$$

In this case, we can assume a steady flow, that means

$$\frac{\partial \vec{B}}{\partial t} = 0 \tag{12}$$

Combining the last two equations, we get $\vec{\nabla} \times \left(\vec{v} \times \vec{B}\right) = 0$.

Now it's time for some simplifications. When calculating $\vec{v} \times \vec{B}$, we find that the resulting vector only has a component in the $\hat{\theta}$ direction: $\vec{v} \times \vec{B} = (0, v_\phi B_r - v_r B_\phi, 0)$.
Applying the curl to this vector, we get

$$\frac{1}{r}\frac{\partial}{\partial r}\left[r\left(v_\phi B_r - v_r B_\phi\right)\right] = 0 \tag{13}$$

which leads to

$$r\left(v_\phi B_r - v_r B_\phi\right) = \text{const.} \tag{14}$$

One can assume that the initial magnetic field emerging from the sun is radial ($B_{\phi_0} = 0$, $B_{r_0} = B_0$), yielding

$$r v_\phi B_r - r v_r B_\phi = r_0 v_{\phi_0} B_0 \tag{15}$$

Now we can replace the initial angular velocity by $v_{\phi_0} = r_0\Omega$ and get $r v_\phi B_r - r v_r B_\phi = r_0^2 \Omega B_0$. Solving for B_ϕ yields

$$B_\phi = \frac{r v_\phi B_r - r_0^2 \Omega B_0}{r v_r} = \frac{v_\phi B_r - r\Omega\left(\frac{r_0}{r}\right)^2 B_0}{v_r} \tag{16}$$

or (using equation (7)):

$$B_\phi = B_r \cdot \frac{v_\phi - r\Omega}{v_r} \tag{17}$$

At large distances from the sun, $r\Omega \gg v_\phi$, which simplifies the equation to

$$B_\phi = -B_r \cdot \frac{r\Omega}{v_r} = -B_0 \cdot \frac{r_0^2 \Omega}{r v_r} \tag{18}$$

(b) We want to calculate the angle δ between B_ϕ and B_r, thus $\tan\delta = \frac{B_\phi}{B_r} = \frac{r\Omega}{v_r}$. A rotation of 2π in 25.05 days yields $\Omega = 2.9 \cdot 10^{-6}\,\mathrm{s}^{-1}$ for the angular velocity of the solar rotation. Filling in the other parameters, we get the final result $\delta = 47.43\,^\circ$.
For large distances from the sun, $r \to \infty$, thus $\tan\delta \to \infty$, which means that $\delta \to 90\,^\circ$.

1.3 Electric power input

The total electric power is estimated as (Power) = (Poynting flux) × (Cross section). The Poynting flux is

$$\vec{S} = \frac{1}{\mu_0}\vec{E} \times \vec{B}. \tag{19}$$

The electric field is, in an ideally conductive medium,

$$\vec{E} = -\vec{v} \times \vec{B}. \tag{20}$$

For the flow speed 400 [km/s] and the magnetic field 5 [nT], the conductive electric field is 2×10^{-3} [V/m]. Hence the Poynting flux is

$$S = \frac{EB}{\mu_0} \tag{21}$$

$$= \frac{2 \times 10^{-3}\,[\mathrm{V/m}] \times 5 \times 10^{-9}\,[\mathrm{T}]}{4\pi \times 10^{-7}\,[\mathrm{H/m}]} \tag{22}$$

$$= \frac{1}{4\pi} \times 10^{-4}\,[\mathrm{W/m^2}]. \tag{23}$$

Note the units $[\mathrm{V\,T\,H^{-1}}] = [\mathrm{J\,m^{-2}\,s^{-1}}] = [\mathrm{W/m^2}]$. The electric power is

$$\begin{aligned} P &= S\pi R^2 && (24)\\ &= \frac{1}{4\pi} \times 10^{-4}\,[\mathrm{W/m^2}] \times \pi \times (10 \times 6400 \times 10^3)^2\,[\mathrm{m^2}] && (25)\\ &= 10.2 \times 10^{10}\,[\mathrm{W}]. && (26) \end{aligned}$$

Therefore the electric power input from the solar wind is of the order of 100 [GW]. For reference, a nuclear reactor provides the electric power typically 100 [MW] to 1 [GW]. In reality it is believed that the power input is dependent on the direction of the interplanetary magnetic field (IMF). The southward IMF is favorable to the dayside reconnection and the power input is larger, whereas for the nourthward IMF the power input is the smallest. The power input is often modelled such that it is sensitive to the IMF angle and maximized at the southward IMF, $P \propto VB^2 \sin^4\theta/2$, where θ is the angle of IMF from the north direction ($\tan\theta = B_{\mathrm{dusk}}/B_{\mathrm{north}}$).

1.4 Induced voltage

The induced voltage can be estimated from Faraday's law of induction:

$$EMF = (\vec{v} \times \vec{B}) \cdot L \tag{27}$$

The orbital speed of the shuttle at 300 km is approximately 7700 m/s, according to:

$$v = \sqrt{\frac{G \cdot M_e}{r}} \tag{28}$$

where G is the gravitational constant ($6.67 \cdot 10^{-11}$), M_e is the mass of the earth ($5.98 \cdot 10^{24}$) and $r = r_e + h$ where r_e is the radius of the earth ($6.4 \cdot 10^6$). We can assume the magnetic field of the earth to be the same at 300 km as on the surface (30-60 μT). The magnetic field of the earth is inclined 11° compared to the rotational axis. The inclination of the shuttle orbit is 28°. As the angle between the shuttle velocity vector and the magnetic field varies we can calculate the max and min value of the induced voltage.

Hence the induced voltage potential along the tether is:

$$7700 \cdot \sin(90 - 28 \pm 11) \cdot 50 \cdot 10^{-6} = 0.11 \text{ and } 0.24\mathrm{V/m} \tag{29}$$

February 2009

Max Planck Institute for Solar System Research
Y. Narita, M. Fränz, N. Krupp with assistants
A. Angsmann, L. Guicking, K. Hallgren, and P. Kobel

Exercise for Sun-Planet Connections (2009) - Part 2

Fluxgate Magnetometer

2.1 Measurement principle

(A) A single coil system with a ferromagnetic rod (e.g. iron, nickel) can detect temporal variation of magnetic field $\partial_t B_x$ (Fig. 1A).

Integrate the induction equation

$$\nabla \times \vec{E} = -\partial_t \vec{B} \tag{1}$$

along the pickup coil line and obtain the voltage at the pickup coil as

$$V = -NS\partial_t B_x, \tag{2}$$

where B_x is the magnetic field component along the rod axis. N is the winding number of the pickup coil, and S is the area of the coil.

(B) Consider a double coil system (Fig. 1B). One coil is used as an excitation, and the other coil is used as a pickup. The excitation coil imposes a large-amplitude sine wave pattern in voltage such that the magnetization of the rod is saturated at every half-period. The excitation field under a background magnetic field is given as

$$H(t) = H_0 + he^{i\omega t} \tag{3}$$

and the induction field $B(t)$ is given by the hysterisis curve (B-H curve) as

$$B(t) = H(t) - H^3(t). \tag{4}$$

Here all the coefficients are neglected for simplicity.

Combine Eq. (2), (3), and (4) and show that the pickup coil senses harmonics of the excitation signal, and most importantly, **the second harmonics is proportional to the external magnetic field** H_0.

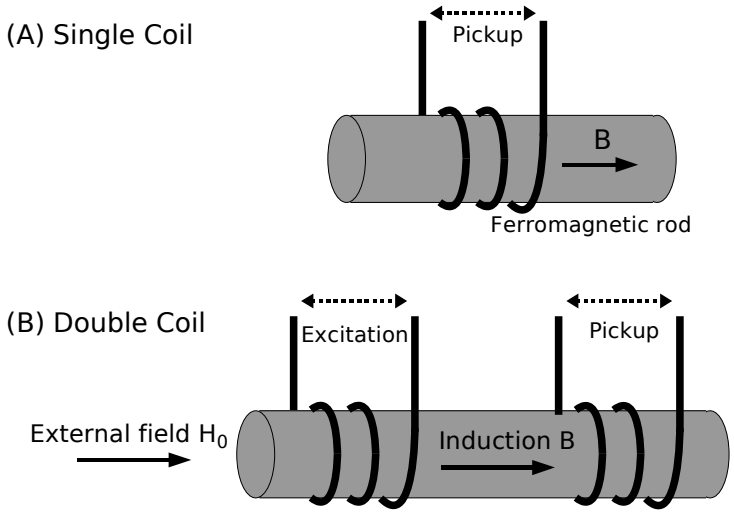

Figure 1: Single and double coil system.

2.2 Assembly

Assemble the four components (Fig. 2) into a fluxgate magnetometer: (1) Ringcore sensor with 2 coil systems ($L_1 = 0.64\,\mathrm{mH}$ and $L_2 = 13\,\mathrm{mH}$); (2) Frequency generator ($f = 8\,\mathrm{kHz}$); (3) Capacitor ($C = x\,\mathrm{nF}$); and (4) Oscilloscope.

- Why do we need a capacitor?
- How much Farad should the capacitor have?

Ringcore sensor is a double coil system with a special geometry to cancel out all the odd harmonics in the pickup signal by its geometrical configuration.

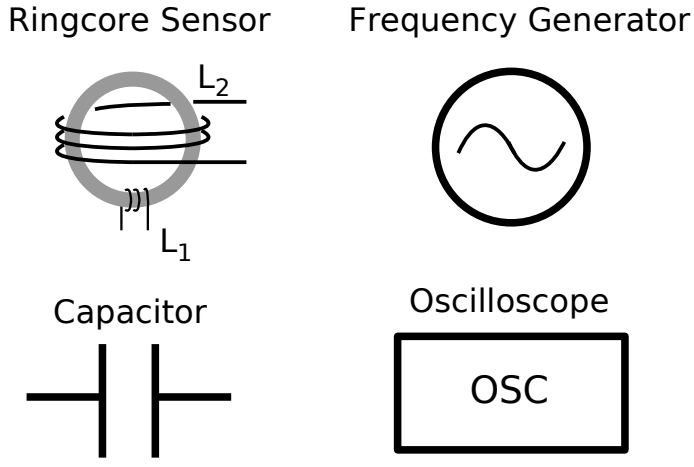

Figure 2: Components for a fluxgate magnetometer.

February 2009

Max Planck Institute for Solar System Research
Y. Narita, M. Fränz, N. Krupp with assistants
A. Angsmann, L. Guicking, K. Hallgren, and P. Kobel

Solutions to Exercise Sun-Planet Connections (2009)

Fluxgate Magnetometer

2.1 Measurement principle

Single coil system

We integrate the induction equation along the coil line,

$$\nabla \times \vec{E} = -\partial_t \vec{B}. \tag{1}$$

The lhs yields the voltage at the pickup coil

$$V = \int (\nabla \times \vec{E}) \cdot d\vec{s}, \tag{2}$$

where $d\vec{s}$ is the line element along the coil. The rhs becomes

$$\begin{aligned} \int (-\partial_t \vec{B}) \cdot d\vec{s} &= -N\partial_t \int \vec{B} \cdot d\vec{s} && (3)\\ &= -N\partial_t \int \vec{B} \cdot d\vec{S} && (4)\\ &= -NS\partial_t B_x. && (5) \end{aligned}$$

Here the Stokes theorem was used and the line integral is replaced by the surface integral. B_x is the magnetic field component along the coil axis, and N and S are the winding number of the coil and the coil area, respectively. The integrated induction equation reads

$$V = -NS\partial_t B_x. \tag{6}$$

Therefore with the single coil system one can determine the magnetic field variation.

Double coil system

The background field can be determined in a double coil system. One coil is used as an excitation and the other is used as a pickup. The excitation coil imposes a sine wave pattern in the magnetic field $H(t)$

$$H(t) = H_0 + he^{i\omega t}, \tag{7}$$

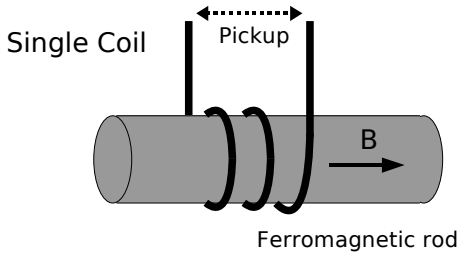

Figure 1: Single coil system.

where the first term on rhs is the background magnetic field (and we aim to measure it), and the second term the excitation part. The excitation is large enough such that the ferromagnetic core is saturated at every half-cycle. The induction field $B(t)$ at the pickup coil is given by the hysterisis curve (B-H curve). For simplicity we approximate the curve as

$$B(t) = H(t) - H^3(t), \tag{8}$$

dropping higher order terms. Using the excitation field $H(t)$ and the B-H curve, the voltage at the pickup coil is given as

$$\begin{aligned} V &= -NS\partial_t B & (9)\\ &= -NS\frac{d}{dt}(H - H^3) & (10)\\ &= -NS[i\omega h(1-3H_0)e^{i\omega t} - i6\omega h^2 H_0 e^{i2\omega t} - i3\omega h^3 e^{i3\omega t}]. & (11) \end{aligned}$$

The output voltage therefore contains harmonics of the excitation signal, $n\omega$, and the second harmonics is proportional to the background magnetic field H_0. If we filter the second harmonics only, the output is

$$V = 6NS\omega h^2 H_0 e^{i2\omega t}. \tag{12}$$

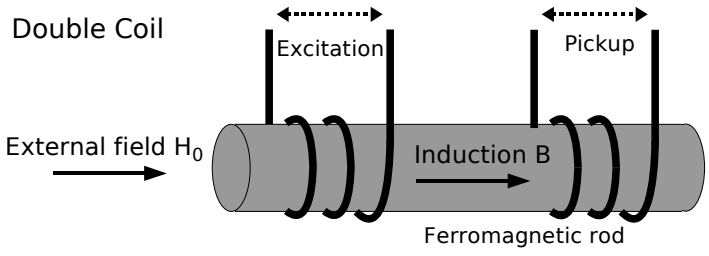

Figure 2: Double coil system.

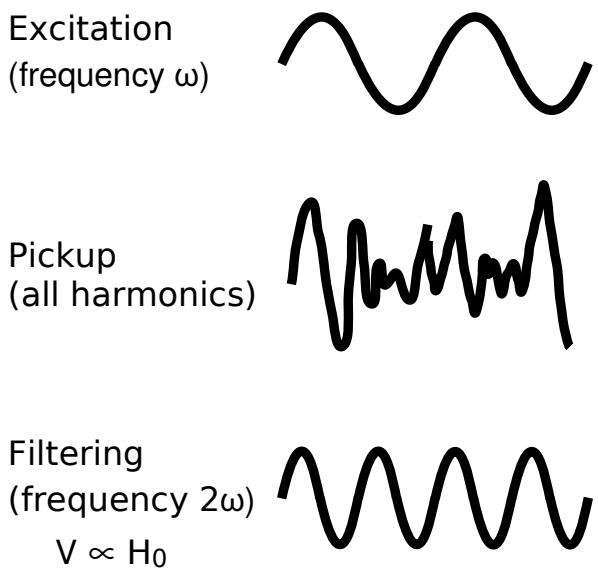

Figure 3: Signal at the excitation, the raw output at the pickup, and the filtered pickup signal.

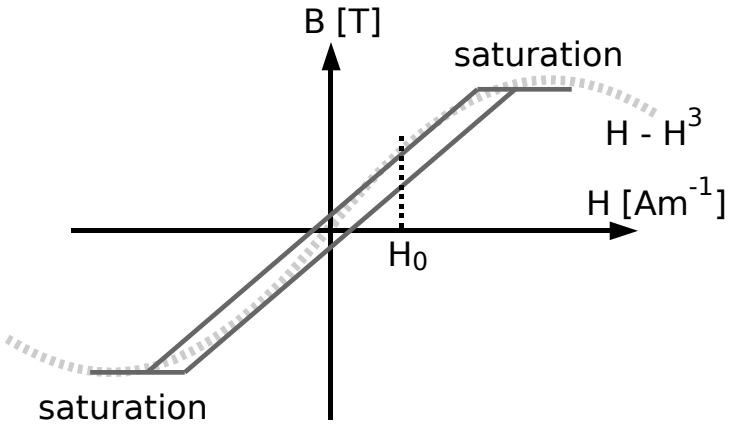

Figure 4: Hysterisis curve of the ferromagnetic rod.

Fluxgate magnetometer

Fluxgate magnetometer is an application of the double coil system. The double rod fluxgate uses two excitation coils in an opposite winding sense, so that all the odd harmonics are canceled out at the pickup. The ringcore fluxgate uses one excitation only, but the ringcore geometry works equivalently as the double rod fluxgate. Excitation frequency is usually in the kHz regime.

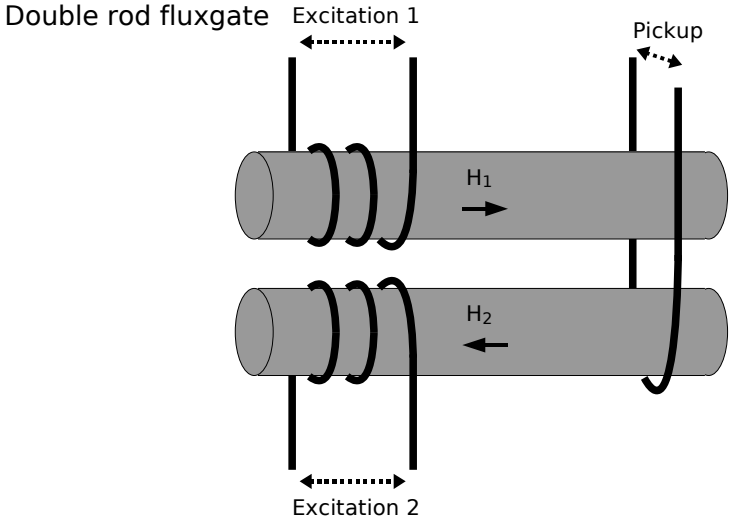

Figure 5: Double rod fluxgate magnetometer.

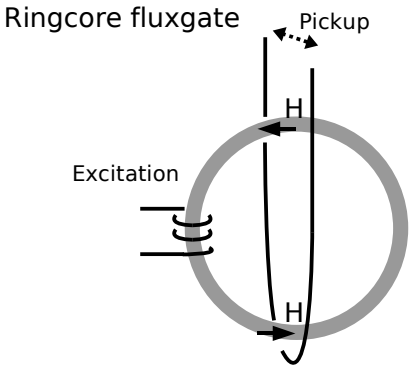

Figure 6: Ringcore fluxgate magnetometer.

2.1 Assembly

The capacitor C is used to form an oscillatory circuit together with the pickup coil L_2. The oscillation frequency is chosen to filter the second harmonics of the excitation frequency $2f$,

$$(2\pi \times 2f)^2 = \frac{1}{L_2 C}. \tag{13}$$

Setting the drive frequency $f = 8\,[\mathrm{kHz}]$ and $L_2 = 13\,[\mathrm{mH}]$, we obtain $C \simeq 8\,[\mathrm{nF}]$.

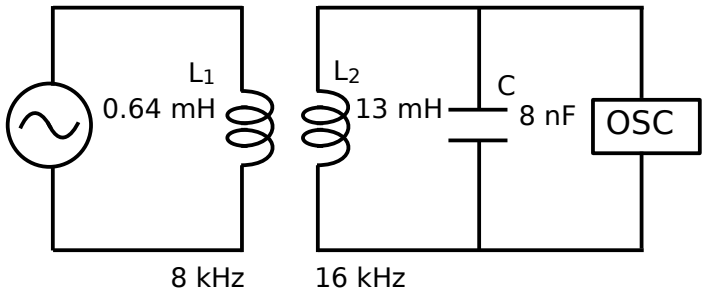

Figure 7: Assembled fluxgate magnetometer.